Structural and Optical Properties of Sn Doped Zinc Oxide (ZnO:Sn) Thin Films Prepared by Spray Pyrolysis Method

Russiarani, S.
Department of Chemistry, Asian College of Engineering and Technology, Coimbatore-641110, Tamil Nadu, INDIA

Krishnaraj, S.
Department of Physics, Periyar Maniammai Institute of Science and Technology, Thanjavur-620024, Tamil Nadu, INDIA

Chandra Mohan, Shanmugavadivelu*[+•]
Division of Phytochemistry, Shanmuga Centre for Medicinal Plants Research, Thanjavur-613007, Tamil Nadu, INDIA

ABSTRACT: *Sn-doped zinc oxide (ZnO:Sn) thin films were deposited onto the ultrasonically cleaned pre-heated glass substrates by employing a simplified spray pyrolysis technique using a spray gun at a constant temperature 250ºC. The films were deposited on the substrate for various solution volumes by taking 0.05M of Zinc acetate as precursor concentration along with 0.0001M & 0.0003M Stannic chloride. The thickness of the films was calculated by the gravimetric weight difference method. The effects of Sn concentration on the structural and optical properties of films were investigated. The deposited films of Sn-doped ZnO showed that the films are c-axis oriented with hexagonal wurtzite structure and preserve their (002) preferential orientation. The grain sizes decreased depending on the increasing Sn concentration. From the optical spectra, all the film exhibits a better transparency of about 80% to 90% in the visible region along with a sharp absorption edge observed which is suitable for optoelectronic applications. The optical band gap slightly increases with increasing Sn doping concentration. The electrical properties of the films show that the resistivity of the film decreases with the increase of Sn concentration with ZnO. The results suggest the potential application of Sn-doped ZnO thin film as a transparent conducting oxide layer for different optoelectronic and photovoltaic devices.*

KEYWORDS: *ZnO thin films; Spray pyrolysis; X-ray diffraction; Optical properties.*

***** *To whom correspondence should be addressed.*
+ *E-mail: cm_123ss@yahoo.co.in*
● *Other Address: Sarvepalli Radhakrishnan University, NH-12, Hoshangabad Road, Jatkhedi, Bhopal, Madhya Pradesh, INDIA*
1021-9986/2023/2/449-460 12/$/6.02

INTRODUCTION

Zinc oxide (ZnO) thin films have wide applications such as light emitting diodes (LED's), laser systems, solar cells, and transparent electrodes, etc., due to their excellent structural and optical properties [1]. These films can be prepared by different techniques, such as Chemical Vapor Deposition (CVD), Pulsed Laser Deposition (PLD) magnetron sputtering, reactive evaporation, spray pyrolysis, etc., [2-4]. Among the methods, the spray pyrolysis technique has several advantages such as simplicity, safety, and low cost of the apparatus and raw materials.

ZnO is a direct large band gap semiconductor and generally, with wurtzite crystal structure [5]. However, the size, the grain orientation, and the quality of the surface depend on the conditions in which the material was prepared and the different treatments that can be made. The surface states of semiconductor materials generate superficial electronic properties which are often affected by their interactions with foreign elements [6].

There are many extensive studies on the crystalline structure and optical transmittance of doped ZnO thin films prepared by spray pyrolysis methods [1,7]. The structural characteristics, electrical and optical properties of the ZnO films have been widely investigated [8], while the doping effect of very low Sn concentration on ZnO thin films and its properties is still under investigation. There are however few studies on optical constants and absorption coefficient of doped ZnO thin films. In the present study, the effect of a very low Sn doping concentration with ZnO in the ratio range of (ZnO:Sn:: 0.05:0.0001M and 0.05: 0.0003M) have investigated the structural and optical properties, and morphology studies of tin-doped zinc oxide thin films deposited by spray pyrolysis technique. Those properties are critically evaluated based on the requirement to be used in organic solar cells.

EXPERIMENTAL SECTION

Sn-doped zinc oxide (ZnO:Sn) thin films were deposited onto the ultrasonically cleaned pre-heated glass substrates by employing a simplified spray pyrolysis technique using a spray gun at a constant temperature 250^{o}C. The deposition parameters employed in this study are tabulated in Table 1. The films were deposited on the substrate for various solution volumes by taking 0.05M of Zinc acetate as precursor concentration along with 0.0001M & 0.0003M Stannic chloride. Several sets of films were fabricated using the same deposition parameters in order to confirm the reproducibility of the films and then characterized. The thickness of the films was calculated by the gravimetric weight difference method. X-Ray Diffraction (XRD) patterns were obtained using X-ray diffractometer (PANalytical PW 340/60 X'pert PRO) which was operated with Cu Kα (λ = 1.5406 Å) radiation. Electrical studies were carried out using a four-point probe and Hall effect apparatus (ECOPIA HMS-3000) with Vander Paw configuration and the transmission spectra of the films were recorded by Perkin Elmer (Lambda 35 model) UV–Vis-NIR double beam spectrophotometer. Photoluminescence spectra were recorded using a Spectro Fluorometer (Jobin Yvon-FLUROLOG-FL3-11) with Xenon Lamp (450W) as the excitation source with a wavelength of 325nm at room temperature. AFM images were obtained using an atomic force microscope (Veeco-di CPII).

Table 1: Process parameters for the deposition of the films.

Spray parameters	Optimum value/ Item
Substrate	Glass
Nozzle - Substrate distance	30 cm
Host Material	Zinc acetate
Dopant Material	Stannic chloride
Solution concentration - ZnO : Sn	0.05M : 0.0001M & 0.05M : 0.0003M
Solvent	Distilled Water
Solution flow rate	5ml / min
Carrier gas	Compressed air
Gas pressure	2 kg/cm^2
Substrate temperature	250 ± 10^{o}C
Angle of spraying	30 - 45^{o}

RESULTS AND DISCUSSION

Structural studies - XRD

Fig.2a and Fig.2b show the XRD pattern of Sn-doped ZnO thin films. The profiles of the XRD structure reveal that the growth of the film is along the c-axis oriented with a hexagonal wurtzite structure. Irrespective of the doping of the Sn concentration all the doped and undoped films have preferential orientation in the same plane (002), indicating that there is no alteration in the preferential growth even in the incorporation of the tin in the Zn sites. In associated with the ZnO (002) plane structure other peaks (101)

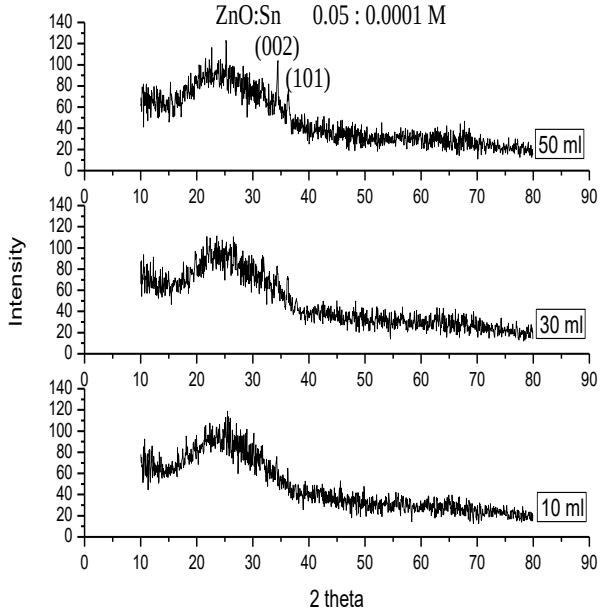

Fig.2a: X-ray diffraction pattern of Sn doped ZnO (0.0001M) thin film deposited on glass substrate at 250°C.

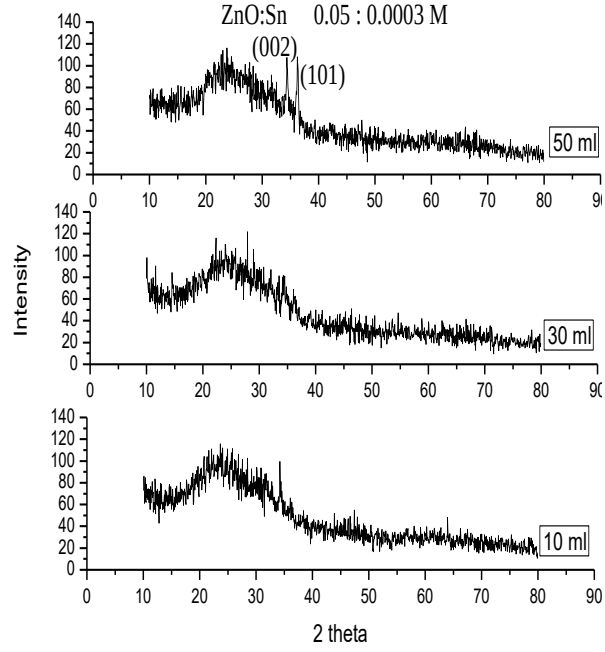

Fig.2b: X-ray diffraction pattern of Sn doped ZnO (0.0003M) thin film deposited on glass substrate at 250°C.

were present. The degree of the preferential growth is gradually declined when the doping concentration varies even though orientation remain as (002) plane.

The texture coefficient (TC) of the doped and undoped ZnO thin film corresponding to the preferential oriented plane (002) is calculated using Eqn. 1

$$TC_{(hkl)} = \frac{I_{(002)} / I_{o(002)}}{1/N\left[\sum_{N} I_{(hkl)} / I_{o(hkl)}\right]} \quad (1)$$

Where $I_{(002)}$ and $I_{o(002)}$ are the measured and the standard relative intensity (JCPDS: 36-1451) values of the (002) plane, $I_{(hkl)}$ and $I_{o(hkl)}$ are the measured relative intensity and standard relative intensity of the hkl plane respectively and N is the number of the diffraction peaks. The TC values of the (002) plane and the variation of the TC as a function of Sn doping concentration in the solution volume of 50ml are shown in Fig.3. From the Fig.3, it is seen that the TC values of (002) plane are slightly decreases with increase of doping concentration, suggesting a monotonically degradation in the crystalline quality of the film due to Sn doping.

The grain size (D) can be estimated using the Scherrer's relation (2). The grain size (D) can be estimated using the Scherrer's relation. [9,10].

$$D = \frac{0.94\,\lambda}{\beta \mathrm{Cos}\theta} \quad (2)$$

Whre λ is the wavelength of X-ray i.e. 1.5405Å, β and Θ are th full-width half maximm and angle ofBraggs diffraction of the 002 diffraction peak respectively, and the crystalline size was estimated for the volume of 30ml and 50ml of the solution are about in nm range are shown in Table 2 and Table 3 for 0.0001M and 0.0003M and their corresponding lattice parameters (a and c) are given in Table 4. For 10ml sprayed solution the film shows the amorphous pattern. The microstrain (ε) and the dislocation density (δ) of films were estimated using Eqs. (3) and (4) [10,11].

$$\varepsilon = \frac{\beta \mathrm{Cot}\theta}{4} \quad (3)$$

$$\delta = \frac{1}{D^2} \quad (4)$$

The XRD pattern of the doped ZnO thin film shows that the (002) peak gets widen along with the gradual decrement of the intensity. A very slight shift right in the 2θ value and the decrement in the c parameters value with the increase of the doping concentration may attribute to the substitutions of Sn^{4+} ions into Zn^{2+} sites. This is arrived because the Sn^{4+} ionic radius (0.069 nm) is less than Zn^{2+}

Table 2: Various parameters of Sn-doped ZnO (0.0001: 0.05) film with different volumes.

Film	The volume of the precursor solution	plane	FWHM	Interplanar distance (d)	Grain size D(nm)	Dislocation Density δ P
ZnO:Sn 0.05: 0.0001M	30 ml	1 0 1	0.3	2.48034E-10	5.5102E-08	3.2935E+14
		0 0 2	1	2.6349E-10	1.6431E-08	3.7039E+15
	50 ml	1 0 1	0.4	2.4724E-10	4.134E-08	5.8511E+14
		0 0 2	0.2	2.6066E-10	8.2239E-08	1.4785E+14

Table 3: Various parameters of Sn doped ZnO (0.0003M : 0.05) film with different volume.

Film	Volume of the precursor solution	Plane	FWHM	Interplanar distance (d)	Grain size D(nm)	Dislocation Density δ P
ZnO:Sn 0.05: 0.0003M	10 ml	0 0 2	0.2	2.6177E-10	8.2206E-08	1.4797E+14
	30 ml	0 0 2	1	2.6199E-10	1.6439E-08	3.6999E+15
	50 ml	0 0 2	0.3	2.6052E-10	5.4829E-08	3.3264E+14

Table 4: Parameters a & c of Sn doped ZnO film of different concentration with different volume.

Temp.	Film	Volume of the precursor solution	0 0 2 Plane		
			Parameters		Strain - ε
			A	C	
250°C	ZnO:Sn 0.05: 0.0001 M	10 ml	-	-	-
		30 ml	3.0015	5.1982	0.004629
		50 ml	3.0137	5.2194	0.000914
	ZnO:Sn 0.05: 0.0003 M	10 ml	3.0270	5.2424	0.0009192
		30 ml	3.0280	5.2442	0.0046005
		50 ml	3.0116	5.2158	0.001371

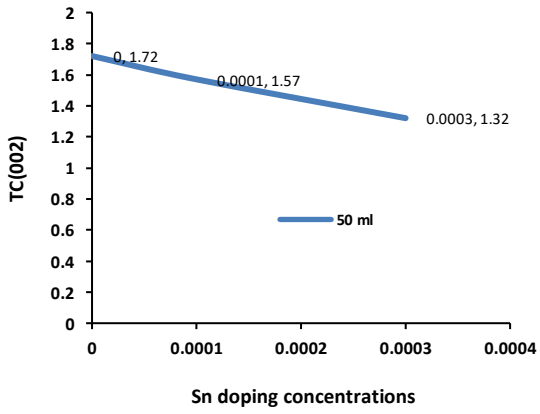

Fig.3: Variation in the TC of 002 plane of ZnO:Sn films.

ionic radius (0.074nm) and hence the substitution of Sn^{4+} into Zn^{2+} sites could cause the slight decrement in the interplanar distance(d).

Here it is observed that the grain size of the film 0.0003M of Sn-doped ZnO at 30 ml volume of solution is less than that of the undoped ZnO film of similar thickness. This is due to the lesser ionic radius of Sn^{+4} (radius = 0.069nm) which substitutes Zn^{+2} (radius = 0.074nm), thereby decreasing the grain size. However, grain size does not vary systematically with Sn dopant concentration, which is attributed to the lattice disorder produced in the films at higher dopant concentrations due to the variation in their ionic radii [12].

Optical studies

The optical transmission and absorption spectra of doped zinc oxide films prepared at a substrate temperature of $250^0 \pm 10^0$C for different Sn doping concentrations (ZnO : Sn :: 0.05 : 0.0001M & 0.05 : 0.0003M) are present in Fig.4(a), 4(b) and Fig.7(a), 7(b). The Evaluations

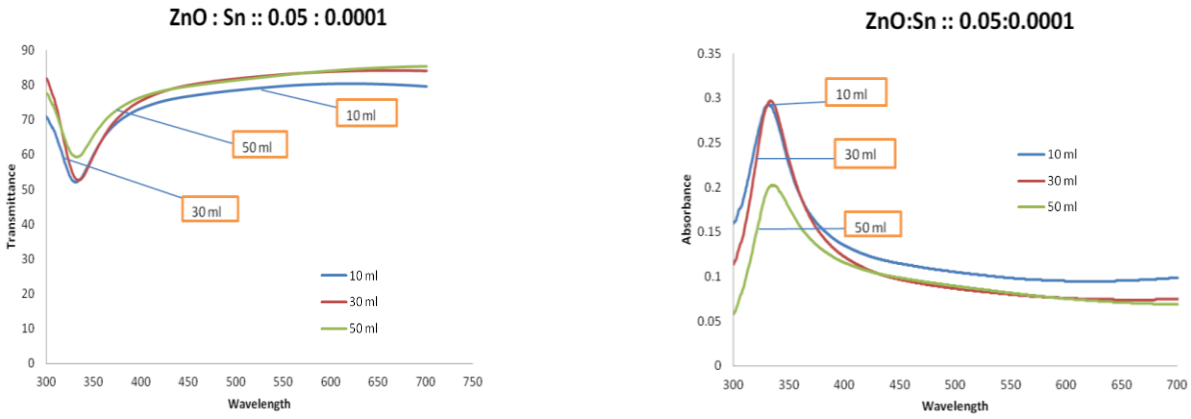

Fig. 4: (a) Transmission spectra of Sn-doped ZnO (0.05:0.0001M) thin films. (b) Absorption spectra of Sn-doped ZnO (0.05 : 0.0001M) thin films.

are made in the wavelength scanning mode under the following parametric conditions:

Incidence - Normal

Temperature - Room temperature

Reference – glass slide (substrate)

Transmission and absorbance spectra of Sn doped ZnO thin films show very low absorbance and high transmittance with increasing doping concentration in the visible region. Transmittance of the film also increases with increase of the volume of the solution at low concentration rather than that of higher concentration. From the spectra, we absorbed that all the film exhibits a better transparency of about 80% to 90% in the visible region along with a sharp absorption edge which is suitable for optoelectronic (solar cell) applications [13]. The optical constants such as refractive index(n) and extinction coefficient(k) were determined from the transmittance spectrum. It is one of the parameters important for optical materials and applications. The variations of refractive index (n) and extinction coefficient (k) with wavelength in the region of 300 nm – 700 nm are shown in Fig. 5(a), 5(b) and Fig. 8(a), 8(b). It shows that the refractive index values in the visible region are varies from 1.5 to 2.0 for undoped and Sn doped ZnO for various volume with different concentrations. This variation in the refractive index is a result of Sn content. Here the extinction coefficient value decreases up to certain values of wavelength and then increased.

The absorption coefficients alpha of ZnO thin films was determined from the measurements of transmittance [14]. If the thickness (t) of the film is known the absorption coefficient (α) can be determined from Eq. (5).

$$\alpha = \frac{\ln(1/T)}{t} \tag{5}$$

The energy gap was determined by using the absorption coefficient values. Fig. 6 and Fig. 9 shows the plot of $(\alpha h\nu)^2$ versus hν, where α is the optical absorption coefficients and hν is the incident photon energy [14, 15]. By assuming a direct transmission between valence band and conduction band the energy gap was estimated using the eqn. 6.

$$\alpha h\nu = K\left(h\nu - E_g\right)^{1/2} \tag{6}$$

The energy gap ' Eg ' is determined and are given in the Table 5. It is found that the *Eg* value is found to be increased with respect to the increase of the Sn doping concentrations.

The optical band gap, estimated by extrapolation of the linear region of the graph to the photon energy axis is found to be increasing from 3.2eV to 3.32eV with dopant concentrations 0.0001 & 0.0003M. The changes in the band gap can be attributed due to the Burstein-Moss band gap widening and band gap narrowing due to electron-electron and electron-impurity scattering. Tailoring the optical bandgap, Eg, of ZnO nanostructured thin films is of great interest to meet increasing demands for diverse practical applications, such as optoelectronics, spintronics, and photonics. Processing parameters, dopant selection, and various combinations of the two have significant

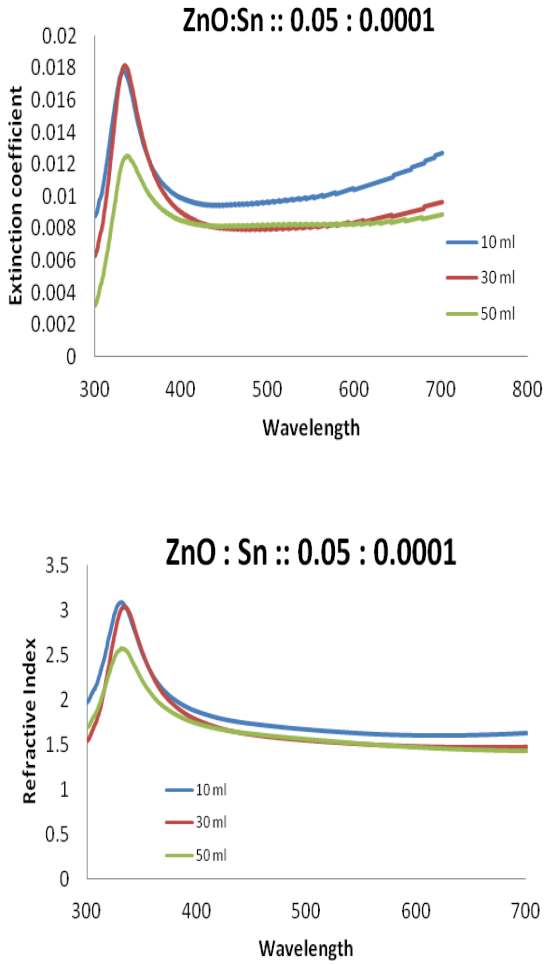

Fig. 5: (a) Extinction coefficients of Sn-doped ZnO (0.05 : 0.0001M) thin films. (b) Refractive index of Sn-doped ZnO (0.05 : 0.0001M) thin films.

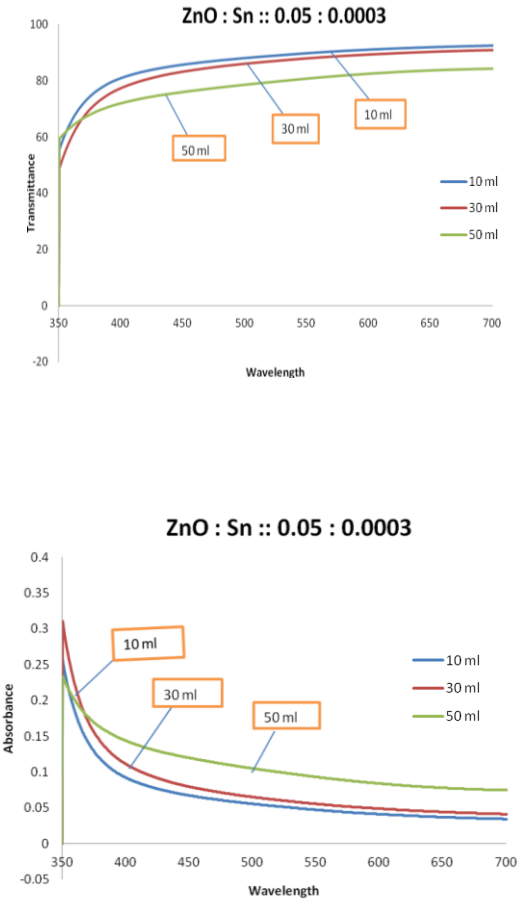

Fig. 7: (a) Transmission spectra of Sn-doped ZnO (0.05 : 0.0003M) thin films. (b) Absorption spectra of Sn-doped ZnO (0.05 : 0.0003M) thin films.

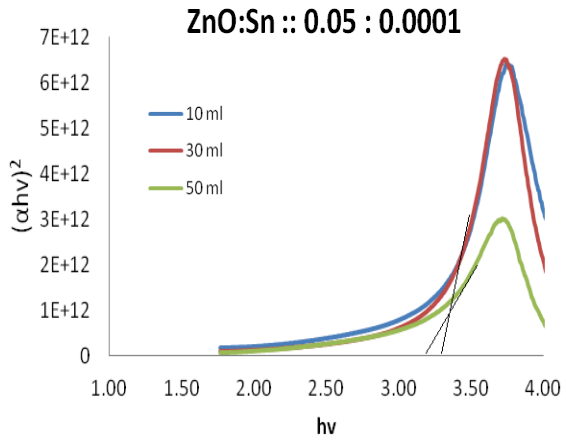

Fig. 6: Band gap of Sn-doped ZnO (0.05: 0.0001M) thin films.

effects on the crystal structure and microstructure of fabricated films, and thus optical performance [16].

Photoluminescence

Fig.10 shows the photoluminescence spectra of Sn-doped and undoped ZnO films at room temperature All the films such as undoped ZnO and Sn-doped (0.0001 & 0.0003M) with two different concentrations shows two distinct emission peaks

1. Sharp UV emission band near 360nm.

2. Green emission spectra in the visible region near 525nm.

It is known that UV band corresponds to the band edge transitions of ZnO and the green emission band relates to defects density [17]. The obtained less intense green

Table 5: Band gap values for undoped and Sn doped ZnO film.

Volume	Band Gap (eV)		
	ZnO	ZnO: Sn-0.0001	ZnO: Sn-0.0003
10	3.28	3.28	3.32
30	3.25	3.28	3.3
50	3.2	3.2	3.24

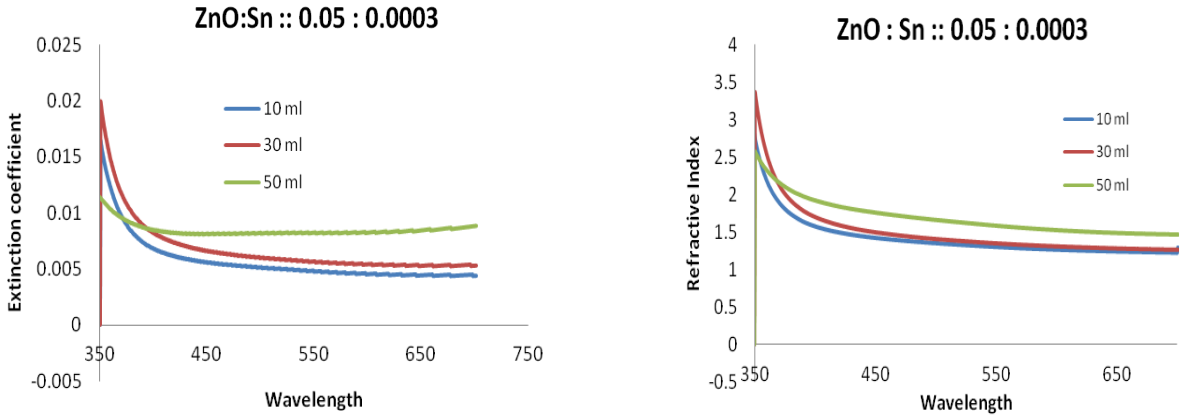

Fig. 4: (a) Extinction coefficients of Sn-doped ZnO (0.05: 0.0003M) thin films. (b) Refractive index of Sn-doped ZnO (0.05 : 0.0003M) thin films.

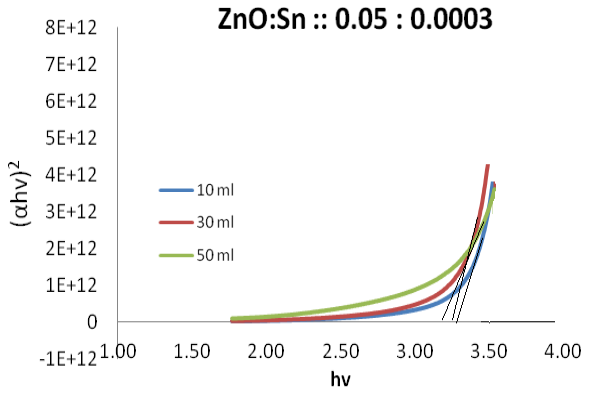

Fig. 9: Band gap of Sn-doped ZnO (0.05: 0.0003M) thin film.

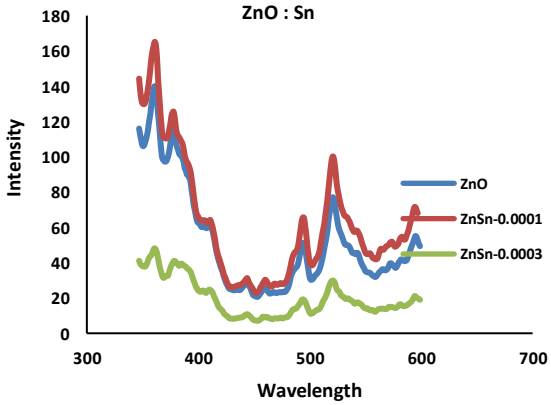

Fig.10: Room temperature photoluminescence spectra of Sn doped ZnO thin film

emission for all the samples indicates the lesser defect concentrations of these films. The shift in the peak towards lower wavelength (blue shift) with increasing intensity of Sn doping concentrations (0.0001M) shows the enhancement of radiative recombination due to the substitution of Sn ions into Zn ions as discussed earlier. This shift in PL spectra corroborates well with the shift of absorption edge absorbed in the transmittance spectra.

Scanning Electron Microscope

SEM images of undoped and Sn doped ZnO thin films on pre heated glass substrates are shown in Fig. 11 and Fig. 12. These images show that the morphology of the films is dependent of the concentration of the Sn dopant. It can be seen that the undoped ZnO film surface exhibits a rough and porous structure. The porous structure is seems to be changed by Sn doping concentrations.

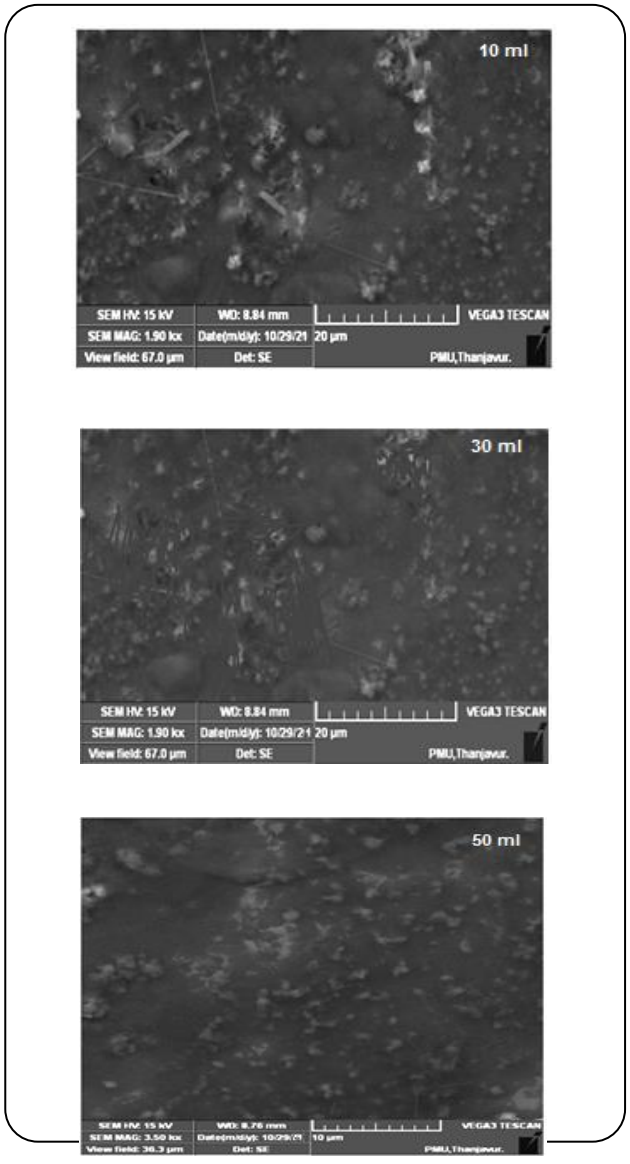

Fig. 11: SEM images of Sn-doped ZnO films (0.0001M).

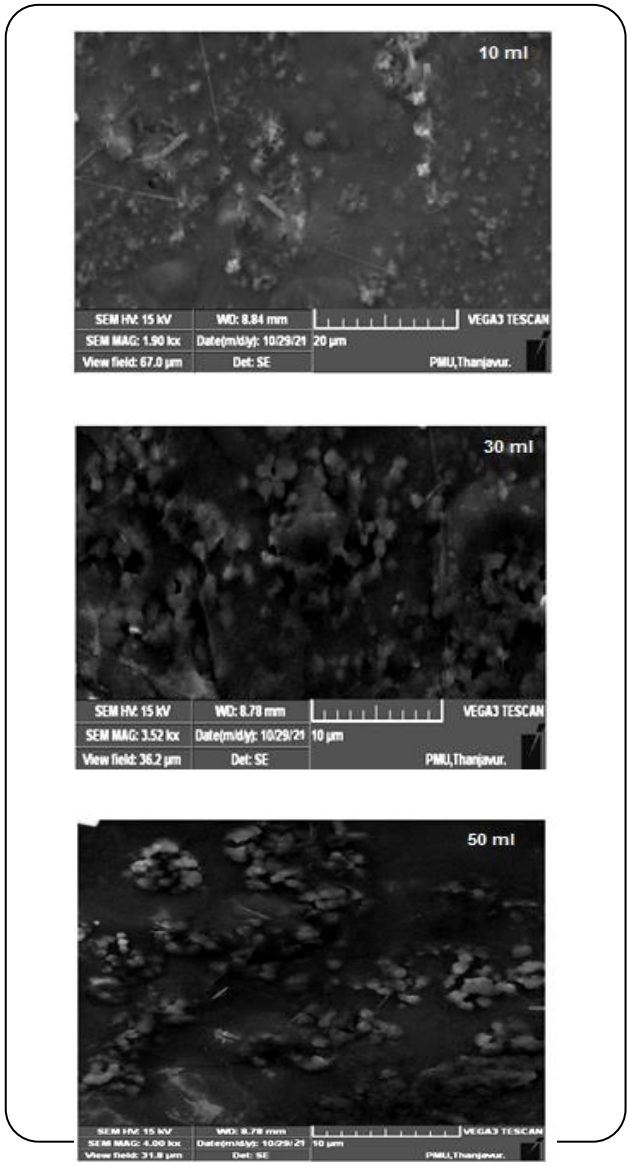

Fig.12: SEM images of Sn-doped ZnO films (0.0003M).

This is expected as the introduction of the stresses due to the difference in ionic radii between Sn and Zn ions causes a reduction in the porous.

Atomic Force Microscopy

Fig.13 and Fig.14 show both 2D and 3D images obtained using an AFM (Atomic Force Microscope) for Sn-doped ZnO films of doping concentrations (0.0001M and 0.0003M) for 50 ml volume of precursor solutions deposited on the glass substrate. The sampling areas used were [5μm × 5μm]. The average roughness values were 4.6nm and 3.45nm.

Table 6 shows the roughness and peak height of the undoped and Sn-doped ZnO thin film. From that, it is observed that the average roughness of the ZnO film is decreased when it is doped with Sn. The roughness of the film is slightly decreased when the concentration increased. ZnO thin film maximum profile peak height is decreased when it is doped with different Sn concentrations and the peak height is decreased with increasing doping concentration. It is worth mentioning that improved quality of the ZnO films such as smoothness, compactness is confirmed by Atomic Force Microscopy (AFM), Scanning Electron Microscopy (SEM) than previous reports [8, 18].

Table 6: Roughness and peak height on the surface of the ZnO : Sn thin film.

Standard Roughness	Undoped ZnO(nm)	Sn Doped ZnO (nm)	
		0.0001M	0.0003M
Average Roughness	14.90	4.60	3.45
Maximum profile peak height	54.36	41.77	9.85
Average maximum profile peak height	27.64	10.52	4.59
Total roughness	88.67	52.93	15.85
Average total roughness	54.84	16.29	8.21

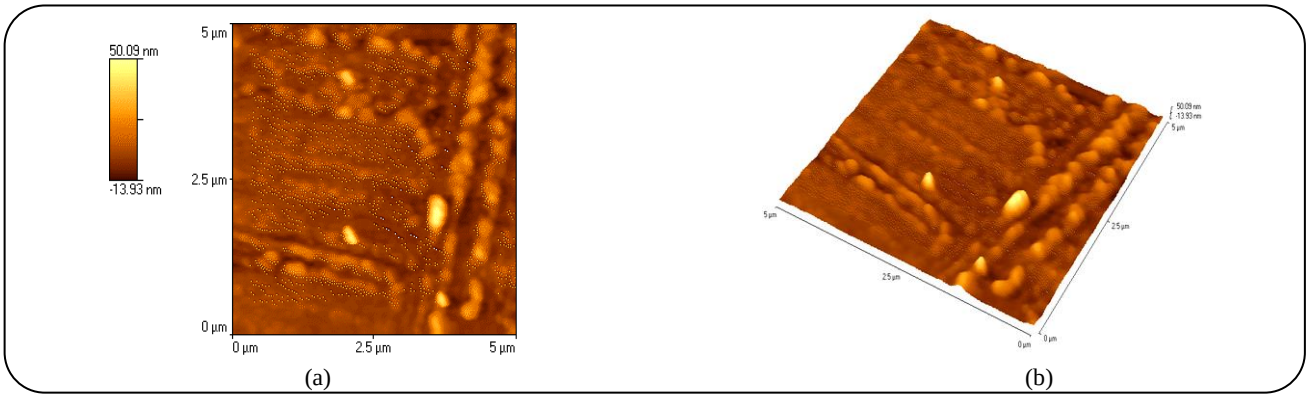

Fig.13: AFM images for Sn doped ZnO (0.0001M) films (a) 2D images, (b) 3D images.

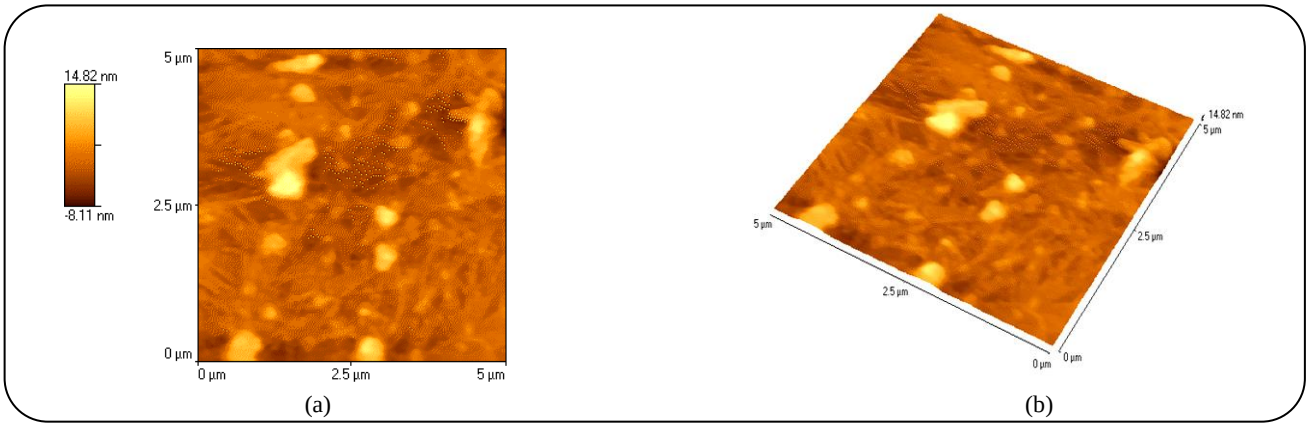

Fig. 14: AFM images for Sn-doped ZnO (0.0003M) films (a) 2D images, (b) 3D images.

Electrical Properties

The Electrical sheet resistance (R_{sh}) of the undoped and Sn doped ZnO thin film for the volume of 50ml precursor solution are shown in Fig.15 and the corresponding resistivity (ρ) of the films is tabulated in Table 7. From Fig.15, it is seen that sheet resistance decreases with the increase of Sn doping concentrations. The decrement of sheet resistance is caused by the substitution of Sn^{4+} ions into the Zn^{2+} sites, each of the ion substitutions results in creation of 2 free electrons. The substitution of tin ion acts as a donor to the system, reducing sheet resistance.

Organic Solar Cells (OSCs) have gained huge attention due to their unique qualities such as lightweight, transparency, flexibility and low-cost [19, 20] Machine learning is a powerful tool, which is based on rapidly growing artificial intelligence technology, is a high-throughput method to accelerate the speed of material design and process optimization. This recognition

Table 7: Electrical parameters of Sn doped ZnO thin film.

Sn doping Concentrations	Resistivity (ρ) x 10^{-4}(Ω Cm)	Sheet Resistance R_{sh} x 10^{2}(Ω/ Cm)
0 M	440	231.58
0.0001 M	286	150.52
0.0003 M	124	65.26

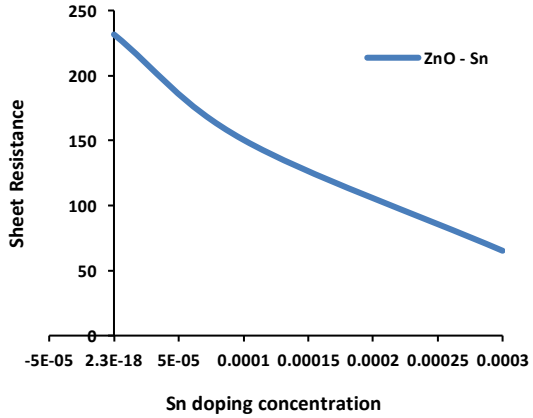

Fig.15: Variation of R_{sh} as a function of Sn doping concentrations.

motivates the present perspective, which focuses on utilizing the experimental data set for machine language to efficiently aid organic solar cell research. Machine learning has a wide scope in organic solar cell research. This is especially useful for complicated problems in material science, such as designing molecules for organic solar cells, which can depend on a vast array of factors and unknown molecular structures. It would take humans years to sift through the data to find the underlying patterns–and even longer to test all of the possible candidate combinations of donor polymers and acceptor molecules that make up an organic solar cell. Thus, progress in improving the efficiency of solar cells like ZnO thin films to be competitive in the renewable energy space has been slow [21-23].

CONCLUSIONS

Sn-doped ZnO thin films were deposited by using an ultrasonic spray technique with a non-aqueous solution. The effects of Sn concentration on the structural and optical properties of films were investigated. The deposited films of Sn-doped ZnO showed that the films are c-axis oriented with hexagonal wurtzite structure and preserve their (002) preferential orientation. The grain sizes decreased depending on the increasing Sn concentration. From the optical spectra we absorbed that all the film exhibits a better transparence of about 80% to 90% in the visible region along with sharp absorption edge which is suitable for optoelectronic applications. The optical band gap slightly increases with increasing Sn doping concentration. The electrical properties of the films show that the resistivity of the film decreases with the increase of Sn concentration with ZnO. The results showed that Sn doping in ZnO thin films markedly decreased the average grain size, the optical transmission and the resistivity, improved the roughness and gave a finer microstructure than that of undoped ZnO thin films.

Received : Jan. 25, 2022 ; Accepted : May 30, 2022

REFERENCES

[1] Chahmat N., Haddad A., Ain-Souya A., Ganfoudi R., Attaf N., Ghers M., Effect of Sn Doping on the Properties of ZnO Thin Films Prepared by Spray Pyrolysis, *J. Mod. Phy.*, **3**(11):1781-1785 (2012). http://dx.doi.org/10.4236/jmp.2012.311222

[2] Fridjine S., Touihri S., Boubaker K., Amlouk M., Belgacem S., Structural and Optical Properties of (ZnO)x (ZnSe)y Thin Films for Optoelectronic Applications, *Phys. Status Solidi C.*, **7(9)**: 2282–2285 (2010). DOI 10.1002/pssc.200983702

[3] Chahmat N., Souier T., Mokri A., Bououdina M., Aida M.S., Ghers M., Structure, Microstructure and Optical Properties of Sn-Doped ZnO Thin Films, *J. Alloys Compd.*, **593**:148-153(2014). https://doi.org/10.1016/j.jallcom.2014.01.024.

[4] Rajasekaran M., Arunachalam A., Kumaresan P., Structural, Morphological and Optical Characterization of Ti Doped ZnO Nanorod Thin Film Synthesized by Spray Pyrolysis Technique, *Mat. Res. Express.*, **7(3)**:036412 (2020). https://iopscience.iop.org/article/10.1088/2053-1591/ ab815d.

[5] Borysiewicz M.A., ZnO as a Functional Material, A Review, *Crystals*, **9(10)**: 505 (2019). https://doi.org/10.3390/cryst9100505

[6] Look D.C., Coskum C., Claflim B., Farlow G.C., Electrical and Optical Properties of Defects and Impurities in Zno, Proceedings of the 22nd International Conference on Defects in Semiconductors, *Physica B: Condensed Mater.*, **340-342**:32-38 (2003). https://doi.org/10.1016/j.physb.2003.09.188.

[7] Lucio-Lópeza M.A., Luna-Arias M.A., Maldonado A., Olvera M. de la L., Acosta D. R., Preparation of Conducting and Transparent Indium-Doped ZnO Thin Films by Chemical Spray, *Sol. Energy Mat. Sol. Cells.*, **90(6)**: 33-741(2006). doi:10.1016/j.solmat.2005.04.010

[8] Ajili M., Castagné M., Turki N.K., Study on the Doping Effect of Sn-doped ZnO Thin Films, *Superlattices Microstruct*., 53:213-222 (2013). https://doi.org/10.1016/j.spmi.2012.10.012

[9] Zak A.K., Majid W.A., Abrishami M., Yousefi R., X-Ray Analysis of ZnO Nanoparticles by Williamson–Hall and Size–Strain Plot Methodsm *Solid State Sci*., **13(1)**: 251–256 (2011). https://doi.org/10.1016/j.solidstatesciences.2010.11.024.

[10] Fu D.-W., Zhang W., Cai H.-L., Ge J.-Z., Zhang Y., Xiong R.-G., Diisopropylammonium Chloride: A Ferroelectric Organic Salt with a High Phase Transition Temperature and Practical Utilization Level of Spontaneous Polarization, *Adv. Mater*., **23(47)**: 5658–5662 (2011). doi: 10.1002/adma.201102938.

[11] Alsaad A.M., Ahmad A.A., Al-Bataineh Q.M., Bani-Salameh A.A., Abdullah H.S., Qattan I.A., Albataineh Z.M., Telfah A.D., Optical, Structural, and Crystal Defects Characterizations of Dip Synthesized (Fe-Ni) Co-Doped ZnO Thin Films, *Materials*, **13(7)**: 1737 (2020). https://doi.org/10.3390/ma13071737

[12] Deng R., Zhang X.T., Effect of Sn Concentration on Structural and Optical Properties of Zinc Oxide Nanobelts, *J. Lumin.*, **128(9)**: 1442-1446(2008). DOI: 10.1016/j.jlumin.2008.01.014

[13] Aleksandrova M, Ivanova T, Strijkova V, Tsanev T, Singh AK, Singh J, Gesheva K. Ga-Doped ZnO Coating—A Suitable Tool for Tuning the Electrode Properties in the Solar Cells with CdS/ZnS Core-Shell Quantum Dots, *Crystals*, **11(2)**:137(2021). https://doi.org/10.3390/cryst11020137

[14] Muchuweni T.S., Sathiaraj H., Nyakotyo, Synthesis and Characterization of Zinc Oxide Thin Films for Optoelectronic Applications, *Heliyon*, **3(4)**: e00285 (2017). https://doi.org/10.1016/j.heliyon.2017.e00285.

[15] Tauc J., Grigorovici R., Vancu A., Optical Properties and Electronic Structure of Amorphous Germanium, *Phys. Stat. Sol.*, **15**: 627-637 (1966). https://doi.org/10.1002/pssb.19660150224

[16] Zhang Y., Xu X., Machine Learning Optical Band Gaps of Doped-ZnO Films, *Optik*, **217**: 164808 (2020). https://doi.org/10.1016/j.ijleo.2020.164808.

[17] Galdámez-Martinez A., Santana G., Güell F., Martínez-Alanis P.R., Dutt A., Photoluminescence of ZnO Nanowires: A Review. *Nanomaterials (Basel)*, **10(5)**: 857 (2020). doi: 10.3390/nano10050857.

[18] Adamopoulos G., Thomas S., Wöbkenberg P.H., Bradley D.D., McLachlan M.A., Anthopoulos T.D., High-Mobility Low-Voltage ZnO and Li-doped ZnO Transistors Based on ZrO_2 High-K Dielectric Grown By Spray Pyrolysis In Ambient Air, *Adv. Mater*., **23(16)**:1894-1898 (2013). DOI: 10.1002/adma.201003935.

[19] Cui, Y., Yao, H., Zhang, J. et al., Over 16% Efficiency Organic Photovoltaic Cells Enabled by a Chlorinated Acceptor with Increased Open-Circuit Voltages, *Nat. Commun*., **10**: 2515 (2019). https://doi.org/10.1038/s41467-019-10351-5

[20] Abdulrazzaq O.A., Saini V., Bourdo, S., Dervishi E., Biris A.S., Organic Solar Cells: A Review of Materials, Limitations, and Possibilities for Improvement, *Part. Sci. Technol*., **31(5)**: 427–442 (2013). https://doi.org/10.1080/02726351.2013.769470

[21] Miyake Y., Saeki A., Machine Learning-Assisted Development of Organic Solar Cell Materials: Issues, Analyses, and Outlooks, *J. Phy. Chem. Lett.*, **12(51)**:12391-12401(2021). DOI: 10.1021/acs.jpclett.1c03526

[22] Mahmood A., Wang J-L., Machine Learning for High Performance Organic Solar Cells: Current Scenario and Future Prospects, *Energy Environ. Sci.*, **14(1)**: 90-105 (2021). DOI:https://doi.org/10.1039/D0EE02838J

[23] Meftahi N., Klymenko M., Christofferson A.J., et al., Machine Learning Property Prediction for Organic Photovoltaic Devices, *npj Comput. Mater.*, **6**:166 (2020). https://doi.org/10.1038/s41524-020-00429-w